Cell Reports, Volume *19*

Supplemental Information

Distinct Corticostriatal GABAergic Neurons Modulate Striatal Output Neurons and Motor Activity

Sarah Melzer, Mariana Gil, David E. Koser, Magdalena Michael, Kee Wui Huang, and Hannah Monyer

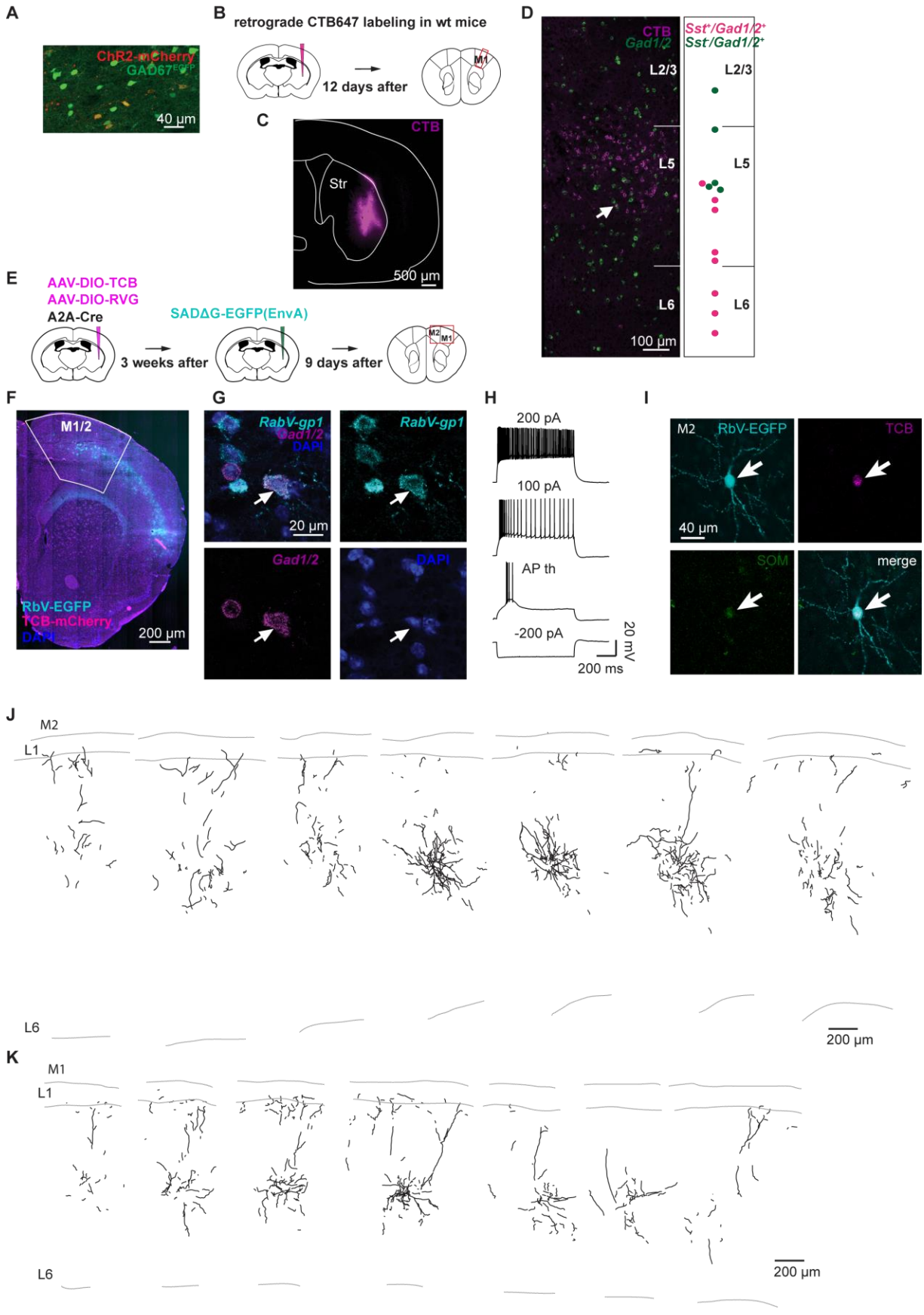
A
ChR2-mCherry
GAD67EGFP
40 µm
B
retrograde CTB647 labeling in wt mice
12 days after
M1
C
CTB
Str
500 µm
D
CTB
Gad1/2
L2/3
L5
L6
100 µm
Sst+/Gad1/2+
Sst-/Gad1/2+
E
AAV-DIO-TCB
AAV-DIO-RVG
A2A-Cre
SADΔG-EGFP(EnvA)
3 weeks after
9 days after
M2
M1
F
M1/2
RbV-EGFP
TCB-mCherry
DAPI
200 µm
G
RabV-gp1
Gad1/2
DAPI
20 µm
H
200 pA
100 pA
AP th
-200 pA
20 mV
200 ms
I
M2
RbV-EGFP
TCB
40 µm
SOM
merge
J
M2
L1
L6
200 µm
K
M1
L1
L6
200 µm

Figure S1 (related to Figure 1)

Martinotti cells in deep layers of motor cortex project to striatum

(A) Confocal image showing mCherry expression in GABAergic neurons following virus-injection into the motor cortex of a $SOM^{Cre}/GAD67^{EGFP}$ mouse.

(B) Schematic drawing indicating injection site of CTB647 in the striatum and site of analysis of retrogradely labeled neurons.

(C) Confocal image showing injection site following injection of the retrograde tracer CTB647 into striatum.

(D) Fluorescent image of cortical layers 2-6 stained with FISH indicating the localization of the retrogradely labeled GABAergic neuron shown in Figure 1D. Approximate borders of layers 2-6 are indicated. Schematic drawing on the right indicates location of all identified SOM^+ and SOM^- retrogradely labeled GABAergic cells in M1.

(E) Schematic drawing showing the protocol steps of transsynaptic labeling employing rabies viruses (SADΔG-EGFP(EnvA)) to reveal corticostriatal GABAergic neurons targeting infected iSPNs.

(F) Injection of Cre-dependent viral constructs encoding TCB-mCherry and rabies glycoprotein into the striatum of A2A-Cre mice followed by injection of SADΔG-EGFP(EnvA) rabies virus into striatum results in typical retrograde labeling (RbV-$EGFP^+$) of cortical neurons mainly in L5. Box indicates area that was screened for retrogradely labeled GABAergic neurons.

(G) Confocal images of a retrogradely labeled GABAergic neuron in motor cortex (arrow) revealed by FISH for *Gad1/2* and rabies mRNA (*RabV-gp1*) after virus injections as depicted in E.

(H) Firing pattern of a burst accommodating SOM^+ projecting neuron identified by retrograde tracing with SADΔG-EGFP(EnvA) rabies virus. TCB was expressed Cre-dependently in the motor cortex of SOM^{Cre} mice and rabies virus was injected into striatum.

(I) Confocal images of a SOM^+ projecting neuron in M2 identified based on its TCB-mCherry, RbV-EGFP and SOM expression after injection of AAV DIO *TCB-mCherry* and SADΔG-EGFP(EnvA) into motor cortex and striatum of SOM^{Cre} mice respectively.

(J) Corresponding morphological reconstruction of the projecting neuron shown in (I).

(K) Reconstructed $SOM^+/TCB^+/EGFP^+$ projecting neuron in M1.

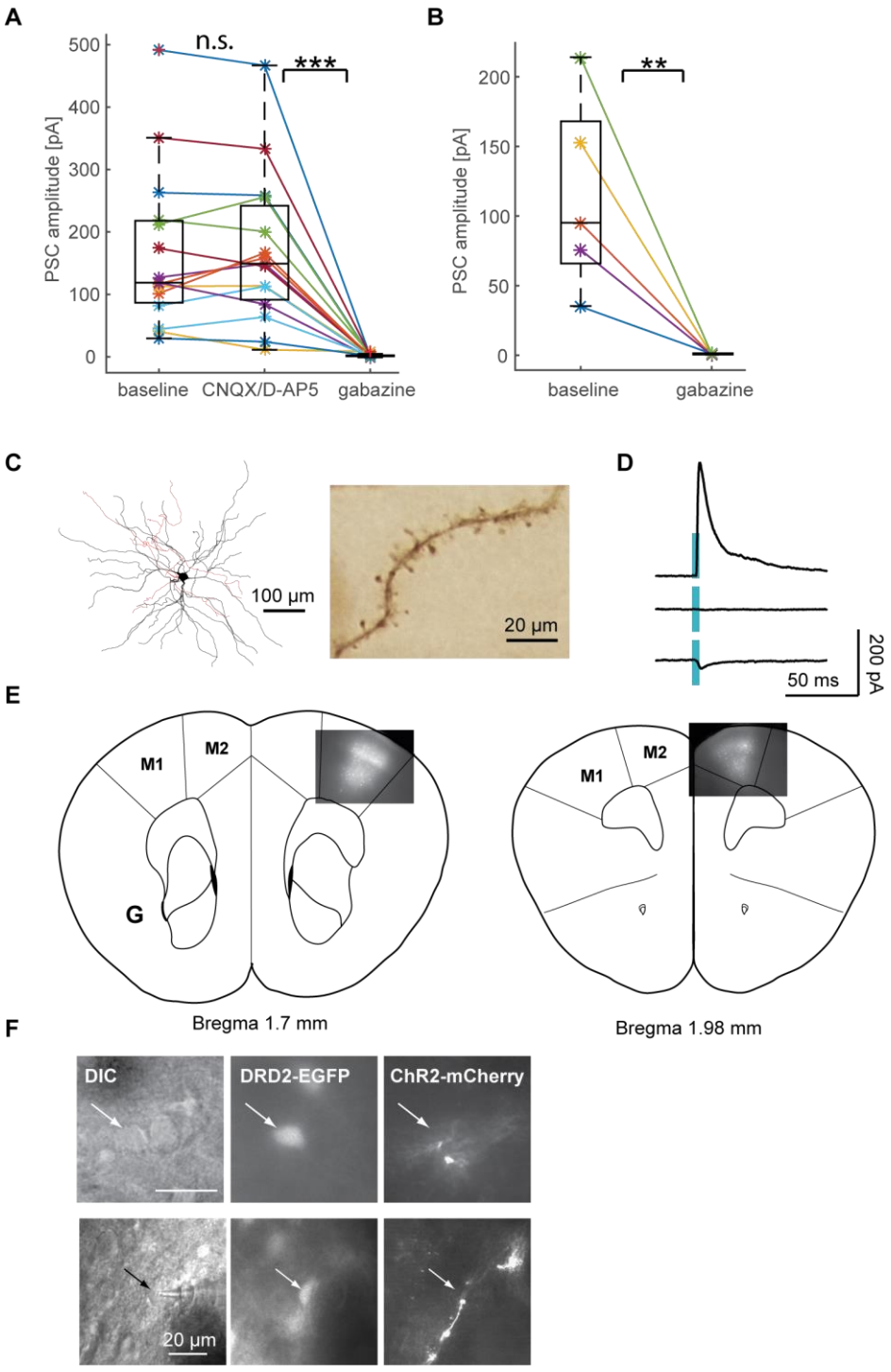

Figure S2 (related to Figure 2)

Long-range SOM$^+$ projections originating in the motor cortex target striatal output neurons and interneurons

(A-B) Dot/box plots (median (IQR), range) indicating the PSC amplitudes of striatal target neurons upon photostimulation of SOM$^+$ projecting neurons before (baseline) and after drug application (CNQX/D-AP5 and gabazine in (A) or only gabazine in (B)). Red crosses indicate outliers. Striatal neurons were patched with either Cs^+

internal solution at a holding potential of +40 mV or with high Cl^- internal solution at a holding potential of -70 mV. Data were pooled since there was no statistical difference between the two conditions.

(C) Representative reconstruction of a responding SPN (axon in red) following photostimulation, and bright field image of dendritic spines.

(D) PSCs of responding GABAergic interneuron at 40 mV, at reversal potential of -75 mV and at -95 mV holding potential with Cs^+ internal solution.

(E) Epifluorescence images of representative M1 (left) and M2 (right) injection sites inserted in schematic drawings of coronal sections.

(F) Exemplary DIC and epifluorescence images of iSPNs that responded to photostimulation and were located in proximity to $mCherry^+$ long-range projections.

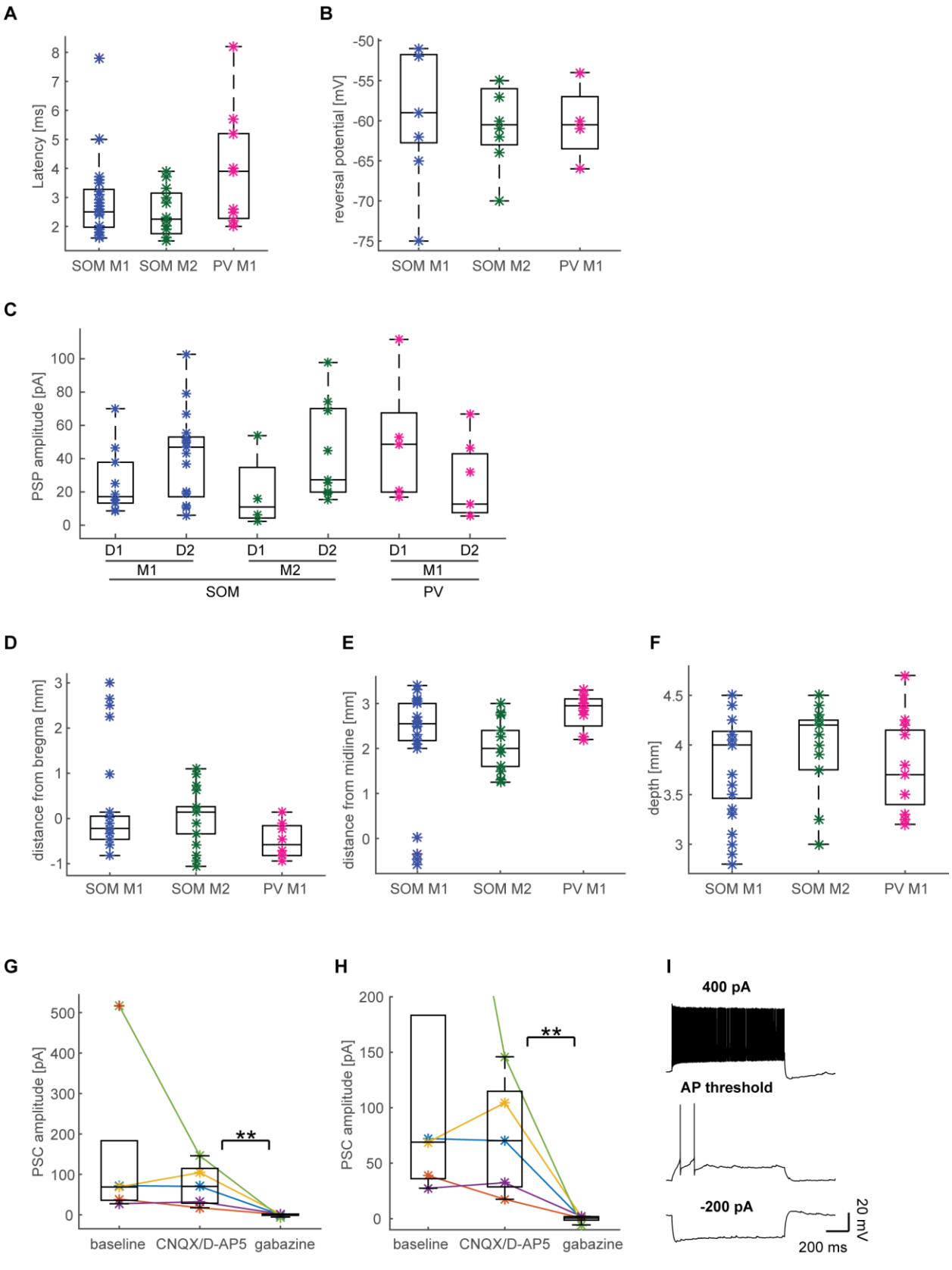
A
Latency [ms]
SOM M1
SOM M2
PV M1
B
reversal potential [mV]
SOM M1
SOM M2
PV M1
C
PSP amplitude [pA]
D1
D2
M1
M2
SOM
PV
D
distance from bregma [mm]
SOM M1
SOM M2
PV M1
E
distance from midline [mm]
SOM M1
SOM M2
PV M1
F
depth [mm]
SOM M1
SOM M2
PV M1
G
PSC amplitude [pA]
**
baseline
CNQX/D-AP5
gabazine
H
PSC amplitude [pA]
**
baseline
CNQX/D-AP5
gabazine
I
400 pA
AP threshold
-200 pA
20 mV
200 ms

Figure S3 (related to Figure 2 and 3)

Responses of SPNs upon stimulation of motor cortex SOM^+ and PV^+ neuron projections are similar

(A-B) Dot/box plots (median (IQR), range) for latency (A) and reversal potential (B) of striatal SPN responses upon photostimulation of primary motor cortex (M1) SOM^+ and PV^+ neuron projections as well as secondary motor cortex (M2) SOM^+ neuron projections.

(C) Dot/box plots for the PSC amplitudes in direct (D1) and indirect (D2) SPNs upon photostimulation of M1 SOM^+ and PV^+ neuron projections as well as M2 SOM^+ neuron projections. Striatal neurons were patched with Cs^+ internal solution and clamped at 0 mV holding potential.

(D-F) Dot/box plots for the coordinates of the localization of responding SPNs in striatum.

(G-H) Dot/box plots indicating the PSC amplitudes of striatal target neurons upon photostimulation of PV^+ neuron projections before (baseline) and after drug (CNQX/D-AP5 and gabazine) application. Striatal neurons were patched with high Cl^- internal solution at a holding potential of -70 mV. Red cross indicates outlier. (H) Magnification of (G) to highlight changes upon gabazine application.

(I) Firing pattern of a fast spiking PV^+ projecting neuron identified by retrograde tracing with SADΔG-EGFP(EnvA) rabies virus. TCB was expressed Cre-dependently in the motor cortex of PV^{Cre} mice and rabies virus was injected into striatum.

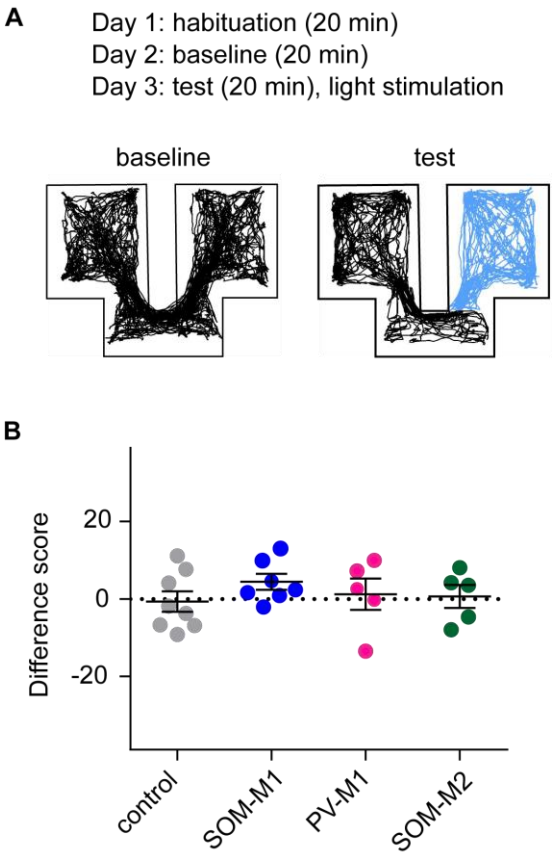

Figure S4 (related to Figure 4)

Stimulation of striatal long-range projections of motor cortex PV$^+$ and SOM$^+$ neurons does not elicit place preference

(A) Exemplary motion traces during baseline and test phases of the light-mediated place preference assay. In the baseline phase, locomotion was measured without photostimulation. During test phase, entering one of the compartments (stimulation side, blue trace) elicited photostimulation.

(B) Mean (± SEM) difference score, as the % of time spent on the 'stimulation' side during baseline minus the % of time spent on the same side during test. Control: n = 8, SOM-M1: n = 7, PV-M1: n = 5, SOM-M2: n = 5 mice.

SUPPLEMENTAL TABLES

Table S1 (related to Figure 1)

Motor cortex SOM$^+$ neurons project to several cortical and subcortical brain areas.

Injection site	Cortical target areas	Subcortical target areas
M1 (n=3)	AI, DI, FrA, GI, M2, S1 DLO, PrL, S2 Cg1/2, Ect, Au2, TeA, LO, LPtA, cl M1, VO	ac, cc, **CPu**, IPAC, LGP acp, ec, ic AA, cg, cl, I, MCLH, MCPO, MGP, rt, Tu, VL, VM, VP
M2 (n=4)	FrA, M1, PrL Cg, DLO, DP,LO, MO, S1, S2, VO AI, cl DP, cl M2, DI, GI, IL, LPtA/MPtA, Pir, V1, V2	cc, **CPu** DTT, LGP, LS, SL, Tu, AAV, cl, ec, HDB, ic, ICj, MGP, MS, Rt, SHi, VDB

Color code indicates areas where labeled projections from M1 and M2 were found in all (magenta), at least 2 (green) or only 1 (blue) injected mouse. The dorsal striatum (CPu, caudate putamen) is highlighted with bold letters. Brain areas were identified based on the Paxinos mouse brain atlas.

Abbreviations cortical areas: **AI**, agranular insular Cx; **Au2**, secondary auditory Cx; **Cg**, cingulate Cx; **cl**, contralateral; **DI**, dysgranular insular Cx; **DLO**, dorsolateral orbitofrontal Cx; **DP**, dorsal peduncular Cx; **Ect**, ectorhinal Cx; **FrA**, frontal association area; **GI**, granular insular Cx; **IL**, infralimbic Cx; **LO**, lateral orbitofrontal Cx; **LPtA**, lateral parietal association Cx; **M1**, primary motor Cx; **M2**, secondary motor cortex; **MO**, medial orbitofrontal Cx; **MPtA**, medial parietal association Cx; **Pir**, piriform Cx; **PrL**, prelimbic Cx; **RSA**, retrosplenial agranular Cx; **S1**, primary somatosensory Cx; **S2**, secondary somatosensory Cx; **TeA**, temporal association Cx; **V1**, primary visual Cx; **V2**, secondary visual Cx; **VO**, ventral orbitofrontal Cx;

Abbreviations subcortical areas: **AA**, anterior amygdaloid area; **AAV**, ventral anterior amygdaloid area; **ac**, anterior commissure; **acp**, anterior commissure, posterior; **cc**, corpus callosum; **cg**, cingulum; **cl**, claustrum; **CPu**, caudate putamen / dorsal striatum; **DTT**, dorsal tenia tecta; **ec**, external capsule; **HDB**, horizontal diagonal band of Broca; **I**, intercalated ncl of the amygdala; **ic**, internal capsule; ICj, island of Calleja; **IPAC**, interstitial nucleus of the posterior limb of the anterior commissure; **LGP**, lateral globus pallidus; **LS**, lateral septum; **MCPO**, magnocellular preoptic ncl; **MGP**, medial globus pallidus; **MS**, medial septum; **Rt**, reticular thalamic ncl; **SHi**, septohippocampal ncl; **SL**, semilunar ncl; **Tu**, olfactory tubercle; **VDB**, ventral diagonal band of Broca; **VL**, ventrolateral thalamic ncl; **VM**, ventromedial thalamic ncl; **VP**, ventral pallidum.

Table S2 (related to Figure 1 and 3)

Firing properties of motor cortex SOM$^+$ and PV$^+$ projecting neurons

	SOM projecting (n = 11)	SOM non-projecting$^-$ (n = 14)	Non-pyramidal PV projecting (n = 3)	Statistics (SOM projecting vs. non-projecting)
V_m [mV]	-63.2 ± 1.6	-66.1 ± 2.1	-63.4 (3.0)	p = 1 $t_{(22)}$ = 1.0
R_i [MOhm]	127.0 (26.4)	136.5 (54.2)	102.9 ± 4.7	p = 1 U = 67
AP_{th} [mV]	-39.3 (3.6)	-38.5 (8.0)	-33.2 (6.8)	p = 1 U = 48.5
Rheobase [pA]	84.0 ± 6.5	144.3 ± 20.5	173.3 ± 40.7	p = 0.12 $t_{(15.6)}$ = 2.8
$AP_{1/2}$ [ms]	0.66 ± 0.04	0.52 ± 0.02	0.37 ± 0.01	p = 0.10 $t_{(12.7)}$ = 3.0
AP_{amp} [mV]	50.1 ± 3.6	54.8 ± 3.1	46.6 ± 2.7	p = 1 $t_{(22)}$ = 1.0
F_{max} [Hz]	120.5 (43.0)	149.5 (84.0)	232.0 (60)	p = 1 U = 38
I_{max} [pA]	342.5 ± 53.8	540 ± 53.1	680 ± 33.5	p = 0.17 $t_{(20)}$ = 2.4
Sag [%]	27.6 ± 5.8	10.2 ± 1.6	17.0 ± 4.9	p = 0.12 $t_{(10.4)}$ = 2.9
Total adaptation [%]	47.9 (28.7)	39.2 (31.3)	34.7 (9.6)	p = 1 U = 42

Retrogradely labeled RbV-EGFP and TCB positive neurons were patched in motor cortex of *SOM^{Cre}* and *PV^{Cre}* mice. Firing patterns were recorded in whole-cell mode with low Cl^- intracellular solution. No statistically significant differences were found between SOM cells that were retrogradely labeled as compared to those that expressed TCB but not RbV-EGFP.

Data are shown as median (IQR) or mean ± SEM. Comparisons were made using Mann-Whitney-U test or unpaired t-test. P-values were corrected for familywise errors using the Holm-Bonferroni test.

Table S3 (Related to Figure 2 and S2)

Electrophysiological properties of target cells and non-targeted SPNs.

	Target SPNs (n = 13)	Non-target SPNs (n = 34)	Cholinergic interneurons (n = 10)	GABAergic interneuron (n = 1)	Statistics (target vs. other SPNs)
V_m [mV]	-79.9 (7.0)	-79.8 (7.7)	-55.2 (9.0)	-63	p = 1 U = 216
R_i [MOhm]	82.0 (34.2)	87.2 (48.6)	181.1 (56.0)	249	p = 1 U = 179
AP_{th} [mV]	-41.0 ± 0.8	-39.2 ± 0.7	-44.6 ± 1.6	43	p = 0.96 $t_{(45)}$ = 1.45
Rheobase [pA]	230 (145)	200 (120)	0 (10)	30	p = 1 U = 196
$AP_{1/2}$ [ms]	0.76 (0.10)	0.85 (0.13)	1.34 (0.40)	0.3	p = 0.48 U = 142
AP_{amp} [mV]	91.5 (9.8)	86.5 (8.8)	71.1 (10.7)	85	p = 0.96 U = 158
F_{max} [Hz]	56.5 ± 6.6	59.7 ± 2.9	20.5 ± 2.4	191	p = 1 $t_{(42)}$ = 0.49
I_{max} [pA]	750 (425)	820 (360)	270 (180)	690	p = 1 U = 180

Cells were patched with high Cl^- intracellular solution. Electrophysiological properties of target and non-target SPNs did not differ. Data are shown as median (IQR) or mean ± SEM. Comparisons were made using Mann-Whitney-U test or unpaired t-test; p-values were corrected for familywise errors using the Holm-Bonferroni test.

Table S4 (Related to Figure 2 and 3)

Response properties and localization of SPNs targeted by M1 and M2 SOM$^+$ and PV$^+$ projecting neurons.

	SOM-M1	SOM-M2	PV-M1	Statistics SOM-M1 vs. SOM-M2	Statistics PV-M1 vs. SOM-M1
Distance from midline [mm]	2.55 (0.8) n = 25	2.0 (0.8) n = 16	3.0 (0.6) n = 12	p = 0.04 U = 142	p = 0.07 U = 95
Distance from bregma [mm]	-0.2 (0.5) n = 25	0.1 (0.6) n = 16	-0.6 (0.7) n = 12	p = 0.3 U = 152	p = 0.02 U = 81
Depth [mm]	4.0 (0.7) n = 25	4.2 (0.5) n = 16	3.7 (0.8) n = 12	p = 0.07 U = 152	p = 0.8 U = 142
Amplitude [pA]	37 (36.6) n = 27	25.4 (41.9) n = 13	26.6 (38.1) n = 12	p = 0.93 U = 172	p = 0.8 U = 152
Latency [ms]	2.5 (1.3) n = 25	2.25 (1.4) n = 12	3.90 (2.93) n = 11	p = 0.4 U = 124	p = 0.08 U = 87
Reversal potential [mV]	58.4 ± 2.7 n = 9	-60.5 ± 1.8 n = 8	-60.3 ± 2.5 n = 4	p = 0.5 $t_{(15)}$ = 0.62	p = 0.7 $t_{(11)}$ = -0.4

Data are shown as median (IQR) or mean ± SEM. Comparisons were made using Mann-Whitney-U test or unpaired t-test.

SUPPLEMENTAL EXPERIMENTAL PROCEDURES

All experiments were performed in 8 to 20 weeks old male *SOM*^{Cre} (Melzer et al., 2012), *PV*^{Cre} (Hippenmeyer et al., 2005), *PV*^{Cre}/GAD67-EGFP (Tamamaki et al., 2003), *SOM*^{Cre}/DRD1a-EGFP, *PV*^{Cre}/DRD1a-EGFP, *SOM*^{Cre}/DRD2-EGFP (Gong et al., 2003) and *PV*^{Cre}/DRD2-EGFP mice with a C57BL/6 background. Animals used for tracing experiments and electrophysiological recordings were group-housed, animals used for behavioral experiments were single-housed. All mice were kept on a 12 h light/dark cycle. All experiments were conducted during the light phase of the schedule.

AAV injections

The pAAV-double floxed-hChR2(H134R)-mCherry-WPRE-pA (AAV DIO *ChR2-mCherry*) vector was obtained from Karl Deisseroth (Cardin et al., 2010). The vector carries an inverted version of Channelrhodopsin2 fused to the fluorescent marker mCherry. In the presence of Cre recombinase, the cassette is inverted into the sense direction, and the fused proteins are expressed from the EF1 promoter. AAV chimeric vectors (virions containing a 1:1 ratio of AAV1 and AAV2 capsid proteins with AAV2 ITRs) were generated as previously described (Klugmann et al., 2005). All rAAVs were stored in undiluted aliquots at a concentration $>10^{12}$ genomic copies per ml at −80° C until intracranial injections were performed.

We injected 8 weeks old male *SOM*^{Cre}, *PV*^{Cre}, *PV*^{Cre}/GAD67-EGFP, *SOM*^{Cre}/DRD1a-EGFP, *PV*^{Cre}/ DRD1a-EGFP, *SOM*^{Cre}/DRD2-EGFP, *PV*^{Cre}/ DRD2-EGFP and *SOM*^{Cre}/*GAD67*^{EGFP} mice. Anesthesia was induced and maintained with isoflurane (1-2.5%). For injections, a small craniotomy (~ 1 mm diameter) was made using the following coordinates (distance from bregma [mm] / distance from midline [mm] / depth [mm] / angle):

Combined primary/secondary motor cortex: 1.8 / 1.5 / 0.7 / 2 degrees towards front

Primary motor cortex: 1.1 / 1.9 / 0.7 / 2 degrees towards front

Secondary motor cortex: 1.6 / 0.8 / 0.6 / 2 degrees towards front

Virus was delivered through a small durotomy by a glass micropipette with a tip resistance of 2 to 4 MOhm. A volume of 100 nl virus (AAV DIO *ChR2-mCherry*) was injected. For more specific injections into primary or secondary motor cortex, 50 nl virus was used. The virus titre was $2x10^{15}$ virus genome/ml, and the pipette held in place for 7 min. The pipette was retracted 50 µm towards the surface, and held in place for another 2 min before complete retraction from the brain. The scalp incision was sutured, and post-surgery analgesics were given to aid recovery (0.03 mg/kg KG Metamizol). Mice were housed for three weeks following the surgery.

Immunohistochemistry

Mice were transcardially perfused with 4% paraformaldehyde (PFA). Coronal and sagittal sections were cut at 50 or 150 µm thickness on a vibratome and washed with phosphate buffered saline (PBS). Free-floating sections were permeabilized and blocked for 2 hrs with PBS containing 5% BSA and 0.2% Triton X-100. Incubation of the sections with primary antibodies was performed for 48 hrs at 4°C. For double-labeling experiments both primary antibodies were incubated simultaneously. Sections were washed with PBS and incubated for 2 hrs with Cy3-conjugated secondary antibody (Jackson Immunoresearch, Newmarket, UK, 1:1000) and/or AlexaFluor488 anti-rabbit secondary antibody (Invitrogen, Darmstadt, Germany, 1:1000) and/or AlexaFluor488 anti-chicken secondary antibody (Life Technologies, Darmstadt, Germany, 1:1000). After repeated washing with PBS, the sections were mounted on 0.1% gelatin-coated glass slides using Mowiol 40-88. Pictures were taken using a BX 51 microscope and a confocal laser-scanning microscope. All injection sites were carefully examined, and mice with labeling of cell bodies in other brain areas were excluded from analysis.

Primary Antibodies

Rabbit anti-somatostatin (Millipore, Temecula CA, 1:1000); rabbit anti-Ds-red (Clontech, Mountain View CA, 1:1000); rabbit anti-EGFP (Invitrogen, Darmstadt, Germany, 1:5000); chicken anti-EGFP (Invitrogen, Darmstadt, Germany, 1:1000); rat anti-somatostatin (Millipore, Temecula CA, 1:500), chicken anti-EGFP (Abcam, Cambridge MA, 1:1000).

DAB staining

Sections were quenched in 1% H_2O_2 for 10 min followed by thorough washing with PBS, before being permeabilized with 1% Triton X-100 in PBS for 1 hr. After repeated washing, sections were incubated with avidin-biotin-horseradish peroxidase complex (Elite ABC, Vector Laboratories, Burlingame CA) in PBS over night at 4°C. After washing with PBS, sections were incubated in a solution containing 0.04% DAB, 49.6% ammonium chloride buffer (0.08% ammonium chloride in PB), and 0.4% glucose oxidase to which 10% beta-D-glucose in H_2O (20 µl/ml) was added one minute after start of the reaction. Sections were kept in the dark for 15-45 min. The reaction was stopped by washing sections again in PBS. Sections were mounted on glass slides using Mowiol 40-88.

Retrograde tracer injection

Seven to10 weeks old wildtype mice were injected into the striatum with 250 nl CTB 647 (4 µg/µl) (Molecular Probes, Eugene, OR). Surgery was as described above. CTB was injected with a flow rate of 100 nl/min using a UMP3 microsyringe pump (World Precision Instruments, Sarasota FL). The pipette was held in place for 10 min before being slowly retracted from the brain within 20 min. The coordinates were (in mm) -2 AP / 2.9 ML / 4 deep with an angle of 30 degrees towards the front. We found that these coordinates were essential to prevent the injection pipette from crossing cortical areas that receive long-range GABAergic inputs from motor cortex, and thus to prevent erroneous labeling of corticocortical GABAergic projecting neurons. 12-14 days after injection mice were sacrificed, sectioned on a cryostat and used for *in situ* hybridization.

Rabies virus tracing

EnvA-pseudotyped, glycoprotein-deleted rabies virus carrying EGFP transgene (SADΔG-EGFP(EnvA)) was generated in house, using starting materials from Byung Kook Lim (UCSD). The recombinant rabies viruses were generated using BHK-B19G and BHK-EnvA cells using protocols similar to those previously described (Wickersham et al., 2010), and were used at a titer of approximately 1.0 x 10^9 infectious units/ml.

Fourteen to 15 weeks old A2A-Cre mice were injected into the striatum with 300-400 nl AAV9 packaged with CAG-Flex-TCB (virus titer $1.5x10^{13}$ gc/ml) encoding the avian virus receptor fused to mCherry, and CAG-Flex-RG ($8.7x10^{13}$ gc/ml) encoding the rabies glycoprotein. Plasmids were a gift from Liqun Luo (Addgene plasmids # 48332 and # 48333). Surgery was as described above. The pipette was held in place for 10 min before being slowly retracted from the brain within another 20 min. The coordinates were (in mm) 0 AP, 2.9 ML, 3.5 deep. 3 weeks later, 400-500 nl rabies viruses were injected in the striatum as described above. Coordinates were either the same as for the AAVs or -2 AP, 2.9 ML, 4 deep with 30 degree angle towards the front. Mice were sacrificed 10 days later and brains were sectioned on a cryostat for subsequent *in situ* hybridization.

To specifically label SOM^+ and PV^+ projecting neurons, we injected 400 nl AAV2/DJ packaged with CAG-Flex-TCB (plasmid as above, virus titer $1x10^{13}$ gc/ml) into the primary and secondary motor cortex (coordinates as above) of SOM^{Cre} ($Sst^{tm2.1(cre)Zjh}$, Jackson Laboratory) and PV^{Cre} mice. The pipette was held in place for 5 min before injecting. AAVs were injected with 50 nl/min flow rate and the pipette retracted 10 min after injection. 2 weeks later, 400 nl SADΔG-EGFP(EnvA) were injected into the striatum with the following coordinates (in mm): -2.6 AP, 2.8 ML 4 and 4.5 deep with 35 degrees angle towards the front. Mice were sacrificed 8-9 days later and used for immuncytochemstry against EGFP and SOM or electrophysiology to characterize electrophysiological parameters of projecting neurons. Since few pyramidal cells were also labeled after injections of the same AAV and rabies virus into C57/BL6 wiltype mice, we assumed that this AAV had Cre-independent 'leak' expression in pyramidal cells, and we thus limited our analysis to cells that had strong TCB-mCherry expression. In SOM^{Cre} mice all patched TCB/$EGFP^+$ cells were non-pyramidal, in PV^{Cre} mice, 1 out of 4 cells had a cell body shape and firing properties of pyramidal cells and was thus excluded from firing pattern analysis.

Three hemispheres of 3 mice were used to exclude that labeling arose from pipette track in cortex. These mice were injected with the same CTB/rabies mixture and the same coordinates except that the rabies injection site was 1.2 mm deep and only 200 nl were injected. No retrograde labeling was observed in the motor cortex of in these mice suggesting that our labeling was specific for striatal injections.

Morphological reconstruction

For morphological reconstruction of projecting neurons, brains were fixed overnight in 4% PFA, coronal slices of 75 µm were cut on a vibratome. Only mice with sparse retrograde labeling (1-2 cells per hemisphere) were used so that

dendrites and axons could be clearly assigned to the reconstructed cell. Slices with retrogradely labeled cell bodies and up to 3 slices anterior and posterior of the cell body were immunostained for EGFP and SOM. In brief, slices were washed in PBS, incubated in PBS with 5% NGS and 0.2% Triton for 1 hr and then incubated at 4°C for 24 hrs with rat anti-SOM and chicken anti-EGFP antibodies. Slices were then washed in PBS with 0.2% Triton, followed by incubation with secondary antibody Alexa 488 anti-chicken and Alexa 647 anti-rat for 1 hr at RT. Slices were washed in PBS with 0.2% Triton followed by PBS.

For morphological reconstructions, only cells that were clearly TCB, EGFP and SOM positive were chosen. Stacks (15 images) of up to 7 consecutive slices surrounding and including the cell body were imaged on a Leica SP8 X confocal microscope using a 20x 0.75 NA oil immersion Leica objective (Leica, Wetzlar, Germany). Tile stack images were merged and maximal intensity projections constructed in Leica Application Suite X software. Cells were reconstructed in Adobe illustrator CS5.

Fluorescent *in situ* hybridization

Mice were deeply anesthetized with isoflurane and decapitated, and their brains were quickly removed and frozen in Tissue Tek OCT compound (VWR, Radnor PA) on dry ice. Brains were cut on a cryostat (Leica CM 1950) into 20 µm sections, adhered to SuperFrost Plus slides (VWR, Radnor PA), and immediately refrozen. Samples were fixed in 4% paraformaldehyde for 15 min at 4 degrees, processed according to RNAscope Fluorescent Multiplex Assay manual (Advanced Cell Diagnostics, Newark CA), and coverslipped with ProLong antifade reagent (Molecular Probes, Eugene, OR). *Gad1* and *Gad2* probes were combined in one channel.

Image analysis

For quantification of retrogradely labeled neurons, 20 µm thick coronal cryostat sections stained with *in situ* hybridization were used. The whole motor cortex of 34 slices was searched for retrograde labeling in rabies virus injected mice using a Leica SP8 X confocal microscope equipped with a 63x 1.4 NA oil immersion objective (Harvard NeuroDiscovery Center). For CTB injected mice, 35 sections were imaged on a Leica SP8 X confocal microscope using a 63x 1.4 NA oil immersion objective (Harvard NeuroDiscovery Center). Per section, one tiled image of 530+/- 10 µm width covering all layers (average are: 530.75 x 1554.06 µm) of the motor cortex was obtained with autofocus, a pixel size of 180 nm and an optical section of 0.9 µm. Imaging sites were chosen such that they were consistent with our anterograde virus injections.

Laser power/intensity for *in vitro* and *in vivo* experiments

Laser power at the optical fiber tip was measured with an optical power meter (POM-110, OZ Optics Ltd., Carp, Canada). For our *in vitro* setup power was ~3.7 mW and for our *in vivo* setup ~3.0 mW. Used fibers were 200 µm in diameter, resulting in a laser intensity (or accurately speaking the irradiance) at the tip of our optic fiber of ~118 mW/mm^2 and ~95 mW/mm^2 for our *in vitro* and *in vivo* setup, respectively. For an estimation of the intensity within the tissue we used: http://web.stanford.edu/group/dlab/cgi-bin/graph/chart.php.

Electrophysiological recordings

For *in vitro* patch-clamp recordings, mice were deeply anesthetized with inhaled isoflurane, and transcardially perfused with ~30 ml ice-cold sucrose solution oxygenated with carbogen gas (95% O2, 5% CO2, pH 7.4). Mice were decapitated and brains removed. 300 µm thick sections were cut on a slicer in ice-cold oxygenated sucrose solution containing (in mM) 252 sucrose, 3 KCl, 1.25 $Na_2H_2PO_4$, 24 $NaHCO_3$, 2 $MgSO_4$, 2 $CaCl_2$, 10 glucose. First, coronal, sagittal and horizontal slices were used. For experiments comparing M1 vs. M2 only coronal slices were used. Slices were incubated in oxygenated Ringer's extracellular solution containing (in mM) 125 mM NaCl, 25 mM $NaHCO_3$, 1.25 mM NaH_2PO4, 2.5 mM KCl, 2 mM $CaCl_2$, 1 mM $MgCl_2$, 25 mM glucose at 32 °C for ~15 min, and subsequently at RT until used for recordings. Whole-cell patch-clamp recordings were performed at 30-32° C using pipettes pulled from borosilicate glass capillaries with resistances of 3-5 MΩ. Sections were continuously perfused with oxygenated extracellular solution. Cells were visualized by an upright microscope equipped with infrared-differential interference contrast and standard epifluorescence.

To investigate synaptic inputs, axonal fibers were stimulated with blue laser light. PSCs were recorded in response to 5 ms photostimulations (473 nm) using approximately 120 mW/mm^2 laser intensity. Glutamatergic and GABAergic synaptic inputs were tested adding via bath-application the following pharmacological agents: Gabazine (10 µM; SR 95531 hydrobromide), D-AP5 (50 µM) and CNQX (10 µM). Amplitudes and latencies of PSCs were measured at 0

mV holding potential using Cs^+-based intracellular solution containing (in mM) 120 Cs^+- gluconate, 10 CsCl, 10 Hepes, 10 phosphocreatine, 8 NaCl, 2 Mg-ATP, 0.3 GTP and 0.2 Hepes, pH 7.3 adjusted with CsOH. FitMaster (HEKA, Lambrecht, Germany) was used for offline analysis of PSCs. In some cases K^+-based, high Cl^- intracellular solution containing (in mM) 127.5 KCl, 11 EGTA, 10 Hepes, 1 $CaCl_2$, 2 $MgCl_2$, 2 Mg-ATP and 0.3 GTP, pH 7.3 adjusted with KOH was used to record firing patterns in targeted cells. In these cases, PSCs were measured at -70 mV holding potential. PSCs were defined as deflections that were time locked to the stimulation and that were larger than the spontaneous fluctuations that occurred during baseline recorded before stimulation after averaging all traces of an experiment. The amplitude is thus measured as difference between amplitude of time-locked deflection and amplitude of spontaneous changes and cells with an amplitude >0 pA were considered as responding. All cells with responses >0 pA were included in the dot plot graphs.

Firing patterns were analyzed in current clamp mode applying 1 s current pulses with 3 s intersweep interval, starting at -50 pA (striatum) or -200 pA (retrogradely labeled cells in motor cortex) and gradually increasing the amplitude in 20 pA steps until saturation was reached. Interpulse interval was set to 3 s. Saturation was defined as a decrease in action potential amplitudes. Firing patterns were analyzed off-line using Matlab. Input resistance was calculated from the steady state voltage step to the first hyperpolarizing current injection for 1 s. Action potential half width was measured at half amplitude of the AP. Maximal frequency was measured at 1000 pA current injection or directly before saturation of the cell. Rheobase was calculated as the minimal injected current that is required to elicit action potentials in whole-cell mode.

For distinction of dSPNs and iSPNs and for comparison of M1 and M2 injections, dSPNs, iSPNs cholinergic and GABAergic interneurons were patched in DRD1a-EGFP and DRD2-EGFP mice cross-bred to either SOM^{Cre} or PV^{Cre} mice. Cholinergic and GABAergic interneurons were patched also in SOM^{Cre} and PV^{Cre} mice since their identification did not require EGFP labeling.

In brief, cell classification into SPNs, cholinergic and GABAergic interneurons in wildtype mice was based on the following characteristics: Cholinergic cells were detected based on their large cell somata, their depolarized resting membrane potential and their slow action potential firing. SPNs and GABAergic interneurons were mostly medium sized and clearly distinguishable from cholinergic cells based on their electrophysiological properties: both cell types are more hyperpolarized and have a higher maximal firing frequency. While GABAergic interneurons can be fast-spiking or non-fast spiking, SPNs are characterized by typical ramp depolarization before action potential initiation, followed by regular action potential firing.

Series resistance was continuously monitored in voltage-clamp mode during PSC recordings measuring peak currents in response to small hyperpolarizing pulses. Series resistances of 37 MOhm were accepted for analyzing PSCs. Stimulus delivery and data acquisition was performed using Pulse software. Signals were filtered at 3 kHz, sampled at 10 kHz. Liquid junction potentials were not corrected.

Biocytin filling and cell reconstruction

For morphological analysis of electrophysiologically identified target cells, whole-cell patch-clamped neurons were filled with biocytin (Aldrich, Taufkirchen, Germany; 10 mg/ml, dissolved in intracellular solution). Cells were filled for up to 30 min before retracting the pipette. The slices with filled cells were fixed overnight in 4% paraformaldehyde and stained with DAB as described above. Labeled cells were reconstructed using Neurolucida software (MicroBrightField, Colchester VT).

Behavioral experiments

Surgery: We bilaterally injected AAV-DIO *ChR2-mCherry* into M1 or M2 of SOM^{Cre} mice and into M1 of PV^{Cre} mice (henceforth, SOM-M1, SOM-M2 and PV-M1 experimental groups, respectively). The control group included: SOM^{Cre} and PV^{Cre} mice injected with AAV1.EF1a.DIO.eYFP.WPRE.hGH (AVV-DIO eYFP) (PennVector, Deisseroth lab) and wildtype litter-mates injected either into the M1 or M2 with AAV-Syn *Tomato* (where the synapsin promoter directs the expression of the fluorescent protein Tomato). Data from these 3 groups of control mice was pooled since no difference in performance was found (data not shown). Viral injections were performed as described above. After injections, we bilaterally implanted optic fiber cannulas (diameter: 200 µm, NA: 0.37, Doric lenses, Quebec, Canada) into the striatum (0.2 mm posterior from bregma, ± 2.8 mm lateral from the midline and 3 mm deep). All mice were male and between 11-17 weeks old when surgery was performed. Mice were single-housed for 3-4 weeks following surgery before behavioral experiments started.

Behavioral set up and protocols: In all experiments, mice were video-tracked at 25 frames per sec and their movements subsequently analyzed using a position tracking system (Ethovision XT9, Noldus). The implanted optic fiber cannulas were connected to two optic fibers attached to a rotary joint (Doric lenses, Quebec, Canada). A patch cord connected the optic fibers to a diode-pumped solid-state 473-nm laser (CrystaLaser, Reno NV). We used a pulse generator (Master 8) and a TTL control box (USB-IO box, Noldus) to automatically control the photostimulation (5 ms pulses delivered at 20 Hz. Laser power, 3 mW).

Evaluation of locomotion activity was performed in a circular arena (40 x 40 cm) placed in a dim lighted room. Animals were allowed to freely run for 21 min. Animals were first recorded for 5 min before any photostimulation. Photostimulation lasted 2 min and was repeated 3 times with an inter-stimulation period of 4 min. The photostimulation protocol can be summarized as follows: 5 min no stimulation, 2 min photostimulation, 4 min no stimulation, 2 min photostimulation, 4 min no stimulation, 2 min photostimulation, 2 min no stimulation. Raw data obtained every 40 ms were processed as follows. We first calculated the distance moved during 5 s (henceforth, "motion"), second we calculated the difference between median motion during and before photostimulation for four epochs of different durations, i.e., 10, 30, 60 and 120 s, starting at photostimulation onset (the median was considered as the data was non normally distributed). Baseline was calculated as the median motion during 120s before photostimulation. For each time epoch we averaged the values obtained during the 3 stimulation periods so that we obtained one single value per mouse. Cumulative frequency histograms as well as mobility and immobility bouts were calculated using the distance moved during 1s windows. Mobility bouts were defined as events in which the average speed (for any 1 s window) was ≥ 1cm/s. Immobility bouts were defined as events in which the average speed (for any 1 s window) was < 1cm/s.

For the place preference task we used a box containing two 20 x 20 x 35 cm compartments connected by a neutral chamber (10 x 20 x 35 cm). Each compartment had distinctive wall patterns (white circles against a black background vs. black circles against a white background). The assay consisted of three 20 min sessions over 3 days. Each session started with the mouse placed into the neutral chamber. We recorded the movements of the mouse inside the two compartments. On day 1, mice were habituated to the apparatus. On day 2 (baseline), no photostimulation was presented. On day 3 (test), one compartment was randomly designated to trigger photostimulation after entry ("stimulation side"). The position of the mouse was calculated in real time using Ethovision software, and this position was used to control the onset of the laser. The sides of the stimulated compartments were counterbalanced across all mice. We first measured the percentage of time spent in each compartment and then calculated a difference score as the percentage of time spent in the "stimulation side" during baseline minus the percentage of time spent on the same side during test (time spent in the neutral chamber connecting both compartments was not considered). A difference score > 0 indicates avoidance of the stimulation side, while a difference score < 0 indicates preference to the stimulation side.

Histology: At the end of the experiments, mice were transcardially perfused with PBS and paraformaldehyde as described above. Brains were dissected and sliced on a vibratome (VT1000s vibratome, Leica, Germany) into 150 µm thick coronal slices. DAB staining was performed as described above to confirm injection and implantation sites.

Statistics

We did not perform blind experiments and did not use statistical methods to predetermine sample size, however, our sample sizes are similar to those generally employed in the field. For electrophysiological data, the Shapiro-Wilk test was used to test for normal distribution. Normally distributed data were then tested for homogeneity of variance using F-tests and data were compared using unpaired t-tests either for equal or unequal variance. Group pairs with at least one non-normally distributed dataset were compared using Mann-Whitney-U tests. Variables for which all groups were normally distributed are shown as mean ± SEM. Variables for which at least one group was non-normally distributed are shown as median (IQR). Proportions of targeted cells were compared using Fisher's exact tests. For pairwise comparisons, paired t-tests (normally distributed data) or Wilcoxon signed rank tests (non-normally distributed data) were used. For multiple pairwise comparisons, Friedman test followed by *post hoc* Conovor's tests (non-normally distributed data) were used. P-values for all multiple electrophysiological and pharmacological data and proportions were corrected with the Holm-Bonferroni test to control for familywise error rates.

For behavioral data, Shapiro-Wilk and Brown-Forsythe tests were used to test normality and homogeneity of variances, respectively. Motion difference for each time window and the difference score were compared across groups using a one-way ANOVA followed by Tukey's multiple comparisons tests. Mobility and immobility bouts before and during photostimulation were compared using paired t-test and Wilcoxon matched-pairs signed rank test.

Graphs were made with Excel (Microsoft), Matlab (The MathWorks) and Prism 6 (GraphPad). The figures were assembled in Illustrator (Adobe) and Inkscape.

The following code was used for p-values in our figures: * < 0.05; ** < 0.01; *** < 0.001.

SUPPLEMENTAL REFERENCES

Cardin, J.A., Carlén, M., Meletis, K., Knoblich, U., Zhang, F., Deisseroth, K., Tsai, L.-H., Moore, C.I., 2010. Targeted optogenetic stimulation and recording of neurons in vivo using cell-type-specific expression of Channelrhodopsin-2. Nat. Protoc. 5, 247–254.

Klugmann, M., Symes, C.W., Leichtlein, C.B., Klaussner, B.K., Dunning, J., Fong, D., Young, D., During, M.J., 2005. AAV-mediated hippocampal expression of short and long Homer 1 proteins differentially affect cognition and seizure activity in adult rats. Mol. Cell. Neurosci. 28, 347–360.

Wickersham, I.R., Sullivan, H.A., Seung, H.S., 2010. Production of glycoprotein-deleted rabies viruses for monosynaptic tracing and high-level gene expression in neurons. Nat. Protoc. 5, 595–606.